

Supporting Information

Positive Magnetic Resonance Angiography by Ultrafine Ferritin-based Iron Oxide

Nanoparticles

Yao Cai^{*,a,b,e}, *Yuqing Wang*^c, *Huangtao Xu*^{a,b,d,e}, *Changqian Cao*^{a,b,e}, *Rixiang Zhu*^e, *Xu Tang*^f,
Tongwei Zhang^{a,b}, *Yongxin Pan*^{*,a,b,d,e}

^aBiogeomagnetism Group, Key Laboratory of Earth and Planetary Physics, Institute of Geology and Geophysics, Chinese Academy of Sciences, Beijing 100029, China;

^bFrance-China International Laboratory of Evolution and Development of Magnetotactic Multicellular Organisms, Chinese Academy of Sciences, Beijing 100029, China;

^cNational Center for Nanoscience and Technology, Beijing 100190, China

^dUniversity of Chinese Academy of Sciences, Beijing 100049, China;

^ePGL, Institute of Geology and Geophysics, Chinese Academy of Sciences; Beijing 100029, China;

^fTransmission Electron Microscope Laboratory, Institutions of Earth Science, Chinese Academy of Sciences, Beijing 100029, China

Keywords: iron oxide nanoparticles, magnetoferritin, T1 contrast agent, magnetic resonance angiography (MRA)

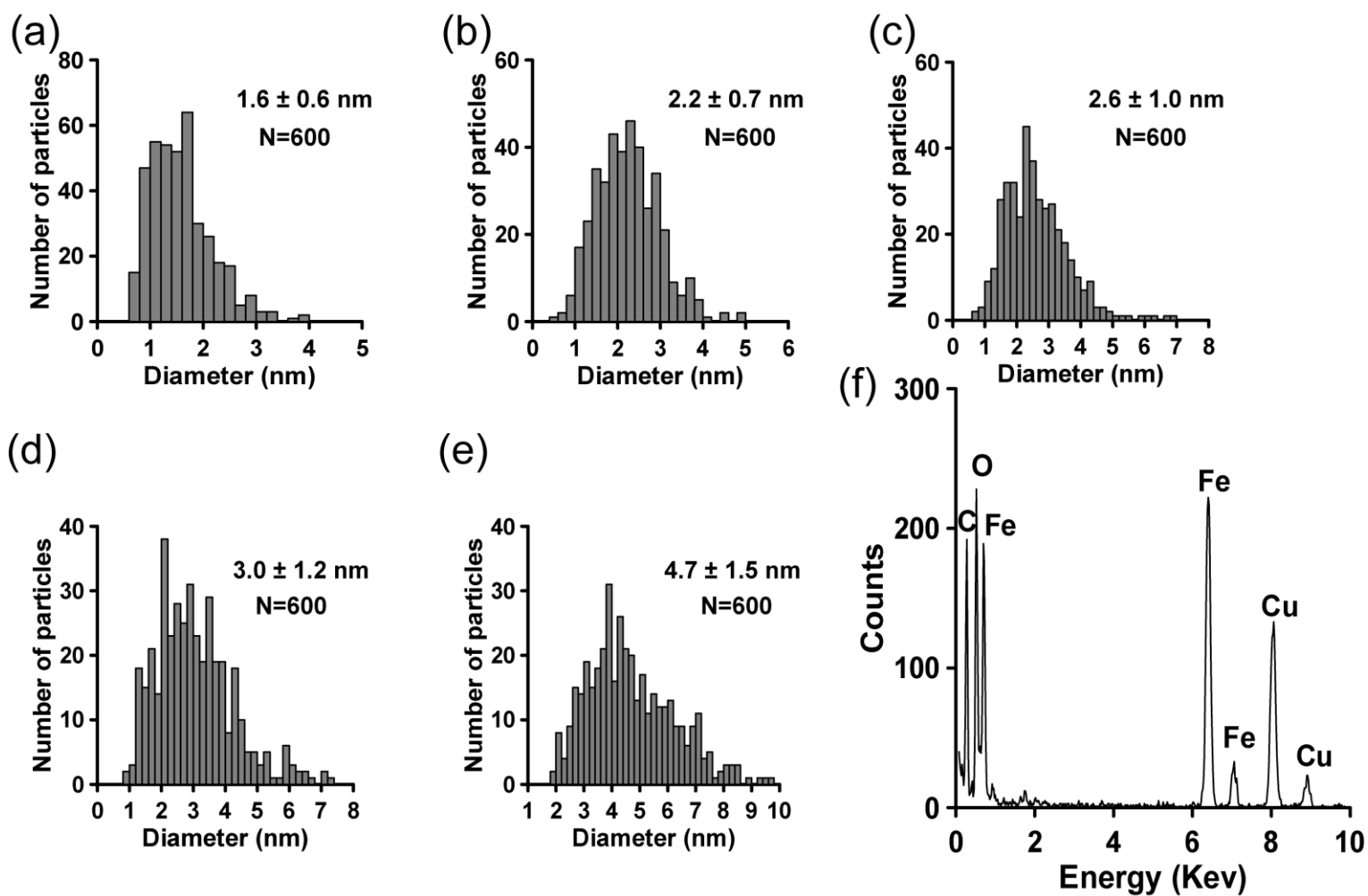


Fig. S1 Histograms of grain-sizes of synthesized M-HFn nanoparticles. Averaged sizes and distribution of iron oxide cores for each sample are results from 600 particles. These samples named as (a) M-HFn-1.6, (b) M-HFn-2.2, (c) M-HFn-2.6, (d) M-HFn-3.0, (e) M-HFn-4.7 and (f) Energy dispersive X-ray spectra (EDS) of M-HFn-2.2.

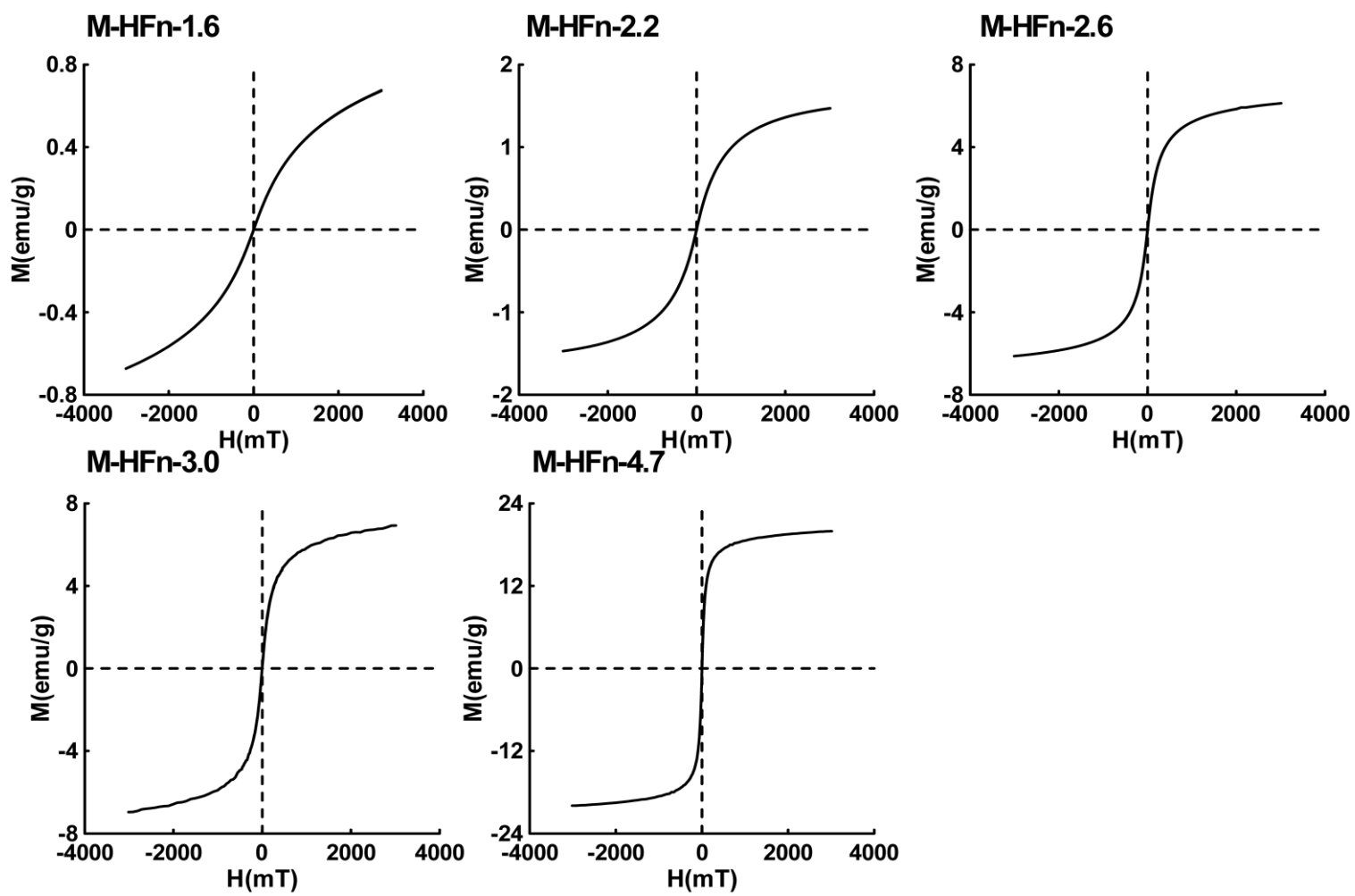


Fig. S2 Room temperature hysteresis loops of M-HFn nanoparticles.

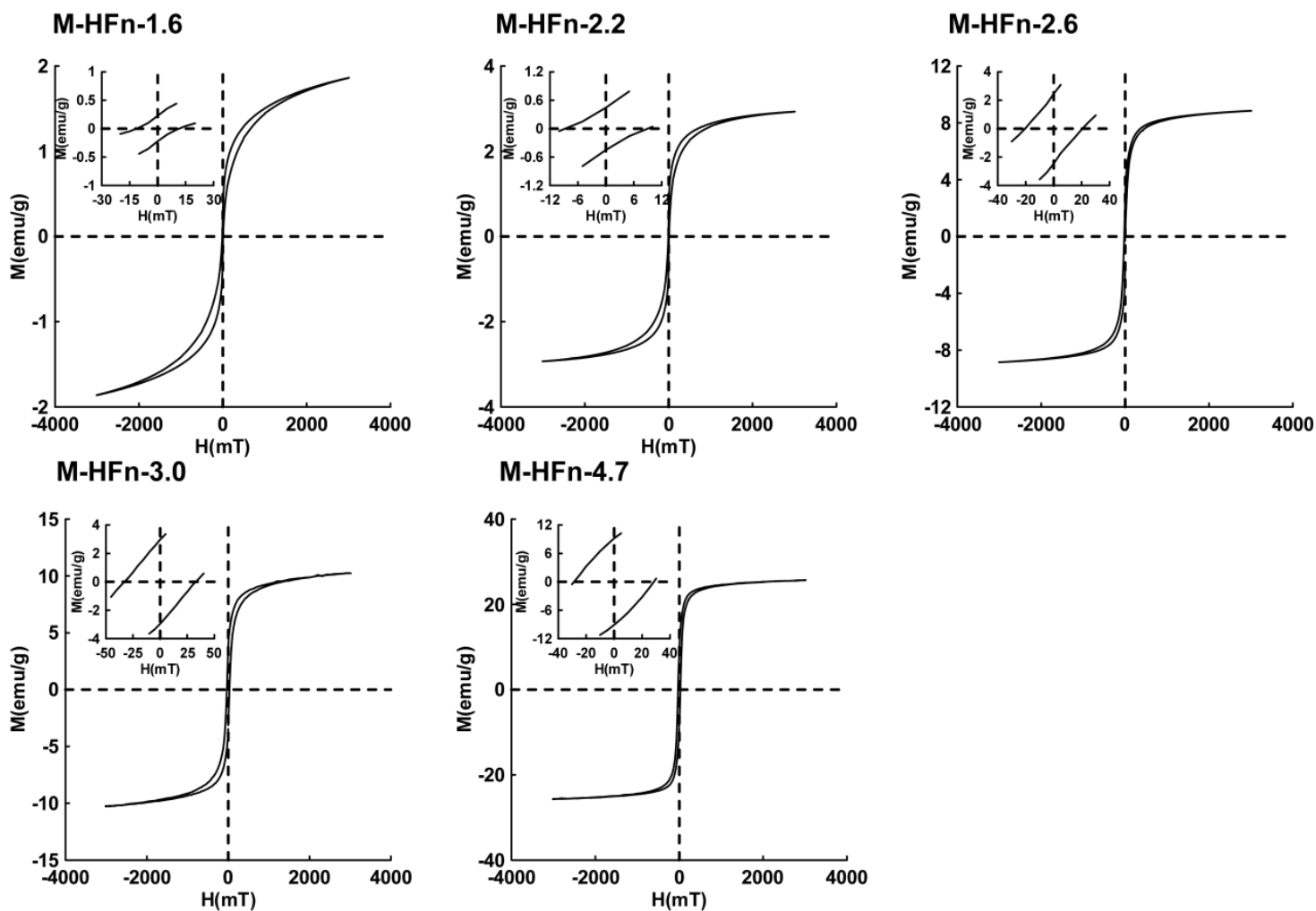


Fig. S3 Hysteresis loops of M-HFn nanoparticles measured at 5 K.

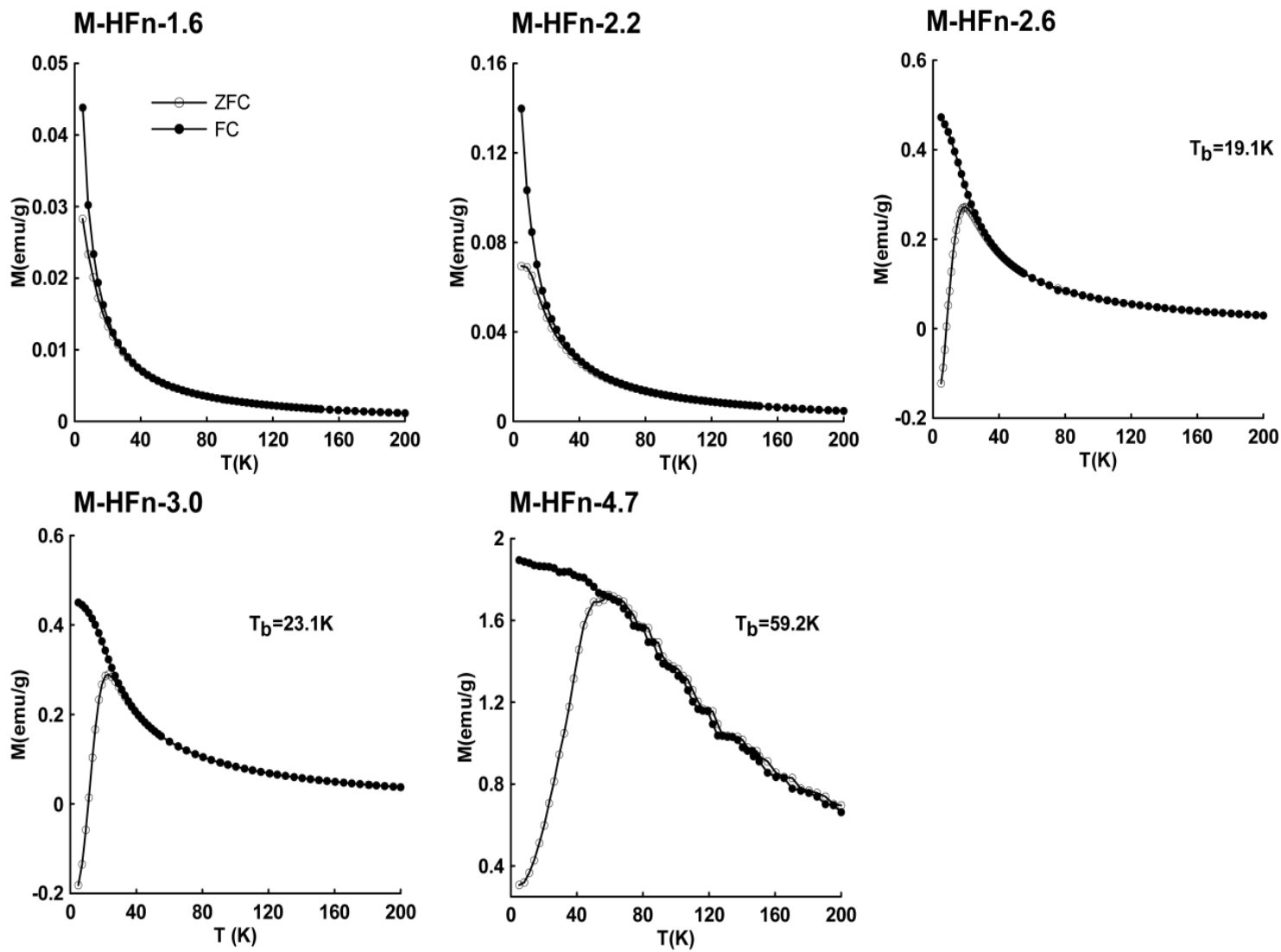


Fig. S4 Low-temperature ZFC (open circle) and FC (filled circle) curves as a function of temperature of M-HFn nanoparticles. T_b , blocking temperature.

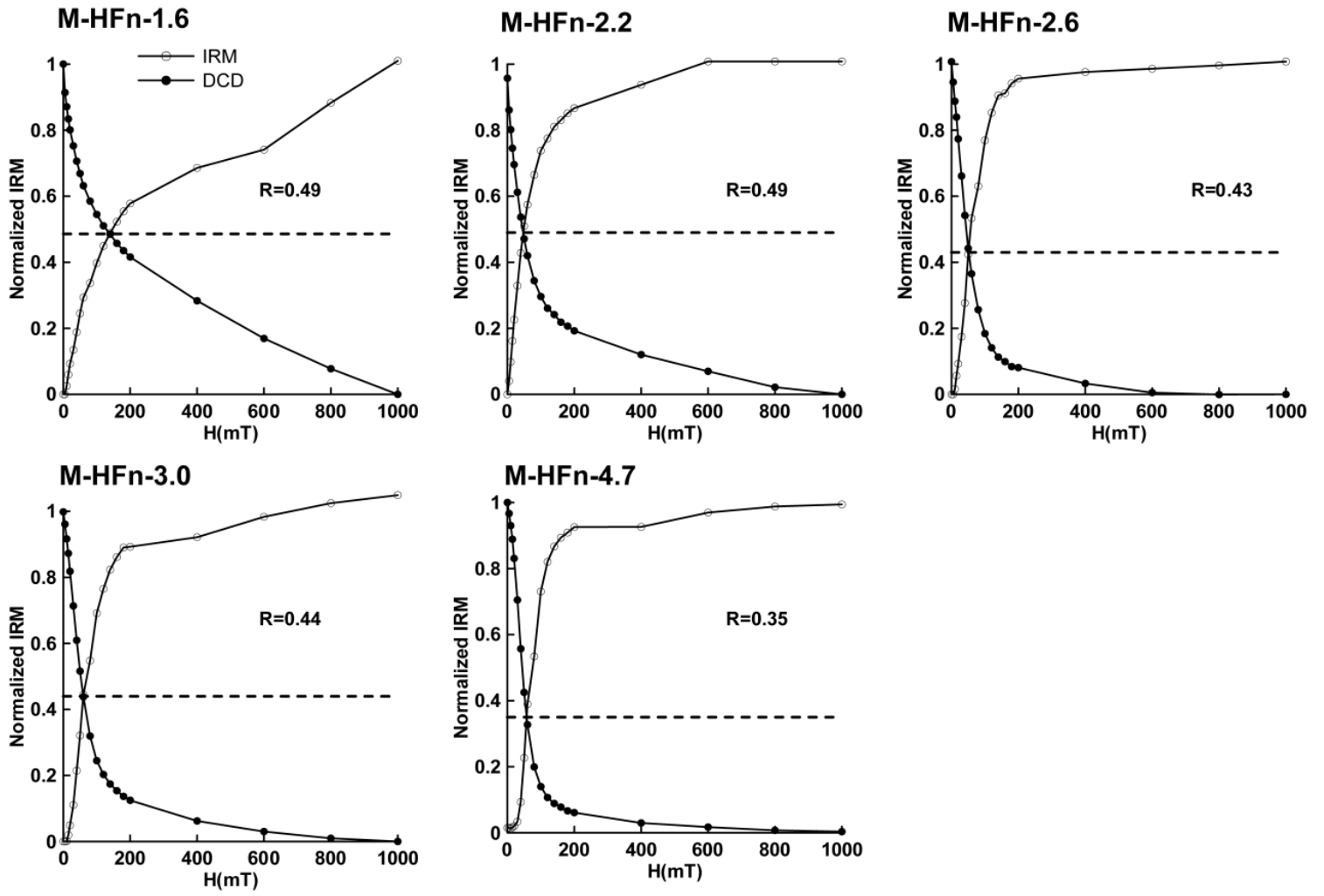


Fig. S5 The Wohlfarth-Cisowski test.

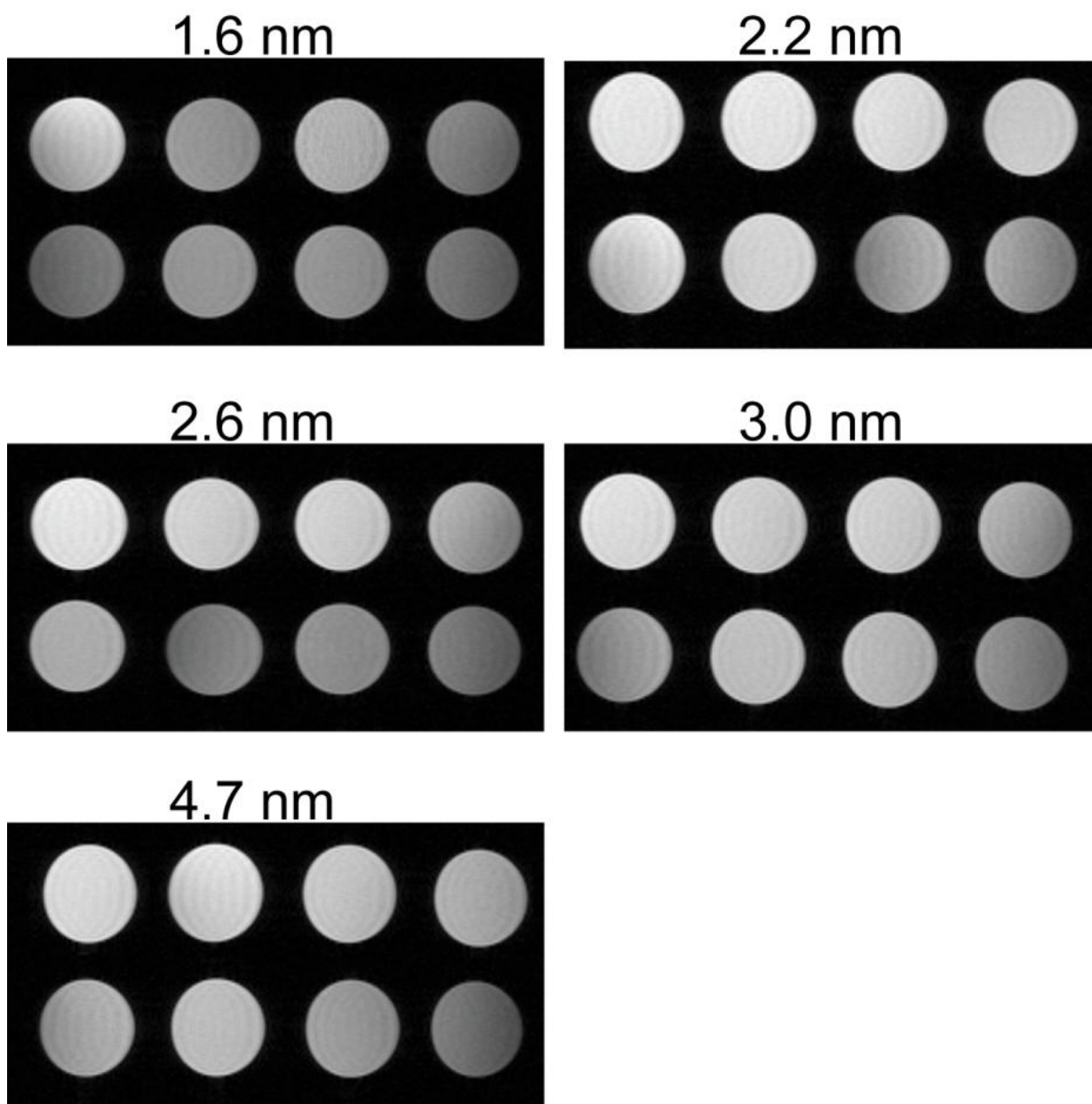


Fig. S6 Evaluation of the T_1 imaging efficiency of M-HFn nanoparticles with different core size.

M-HFn was diluted by different iron concentrations in phosphate buffered saline (from right to left in the lower row are 0, 0.4, 0.6, 0.8 mM; from right to left in the upper row are 1, 1.2, 1.4, 2 mM).

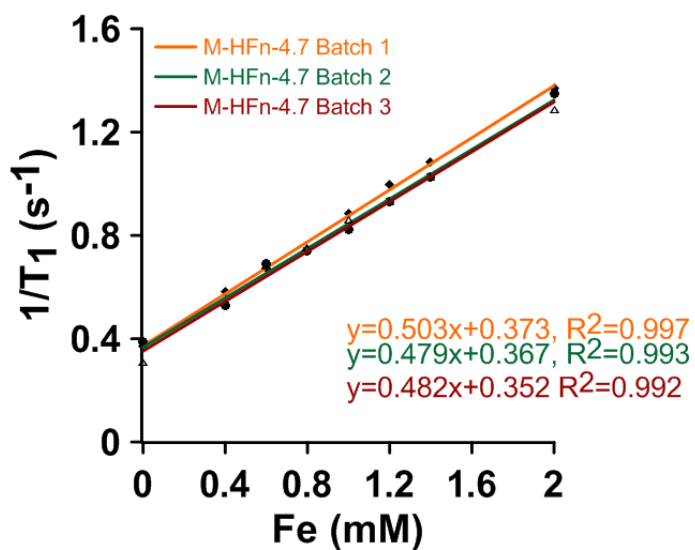
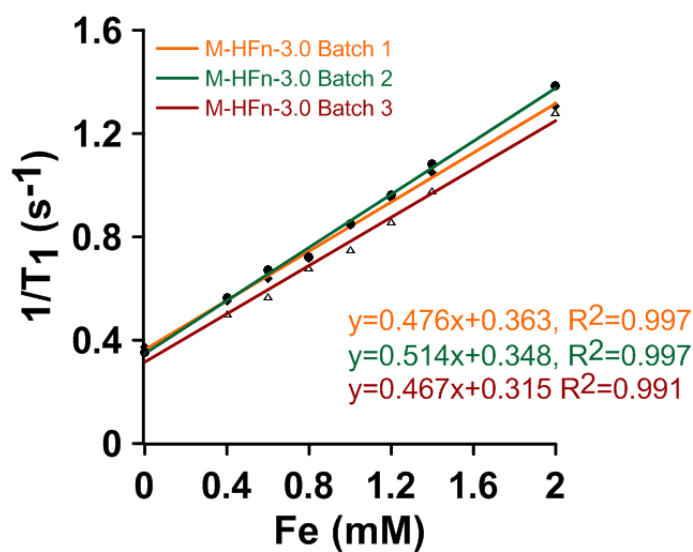
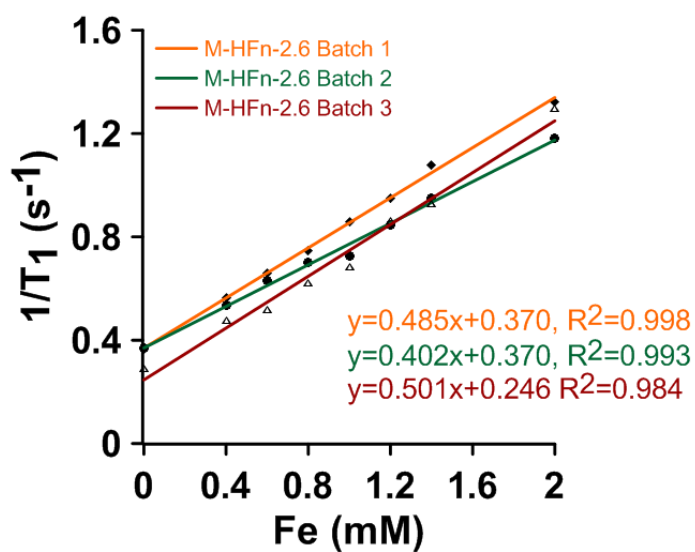
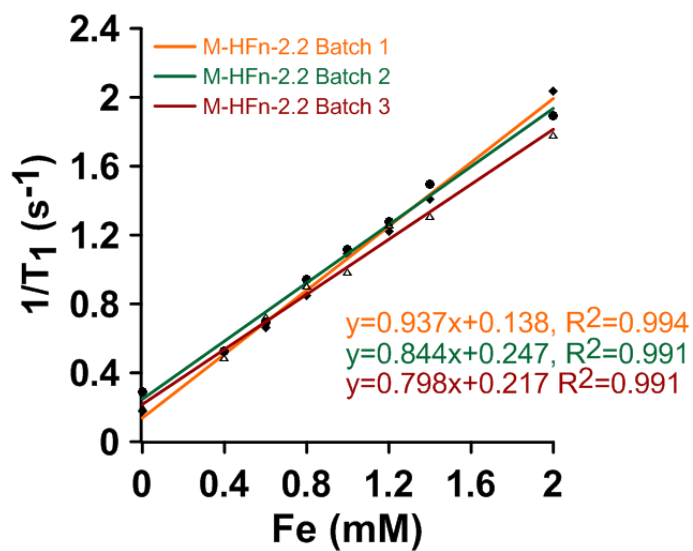
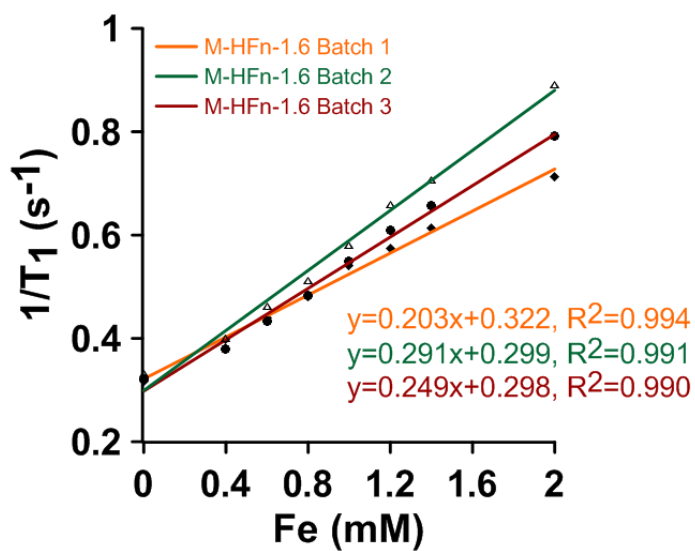


Fig. S7 Analysis of r_1 relaxivity of M-HFn nanoparticles by linear mapping iron concentration and relaxation rate.

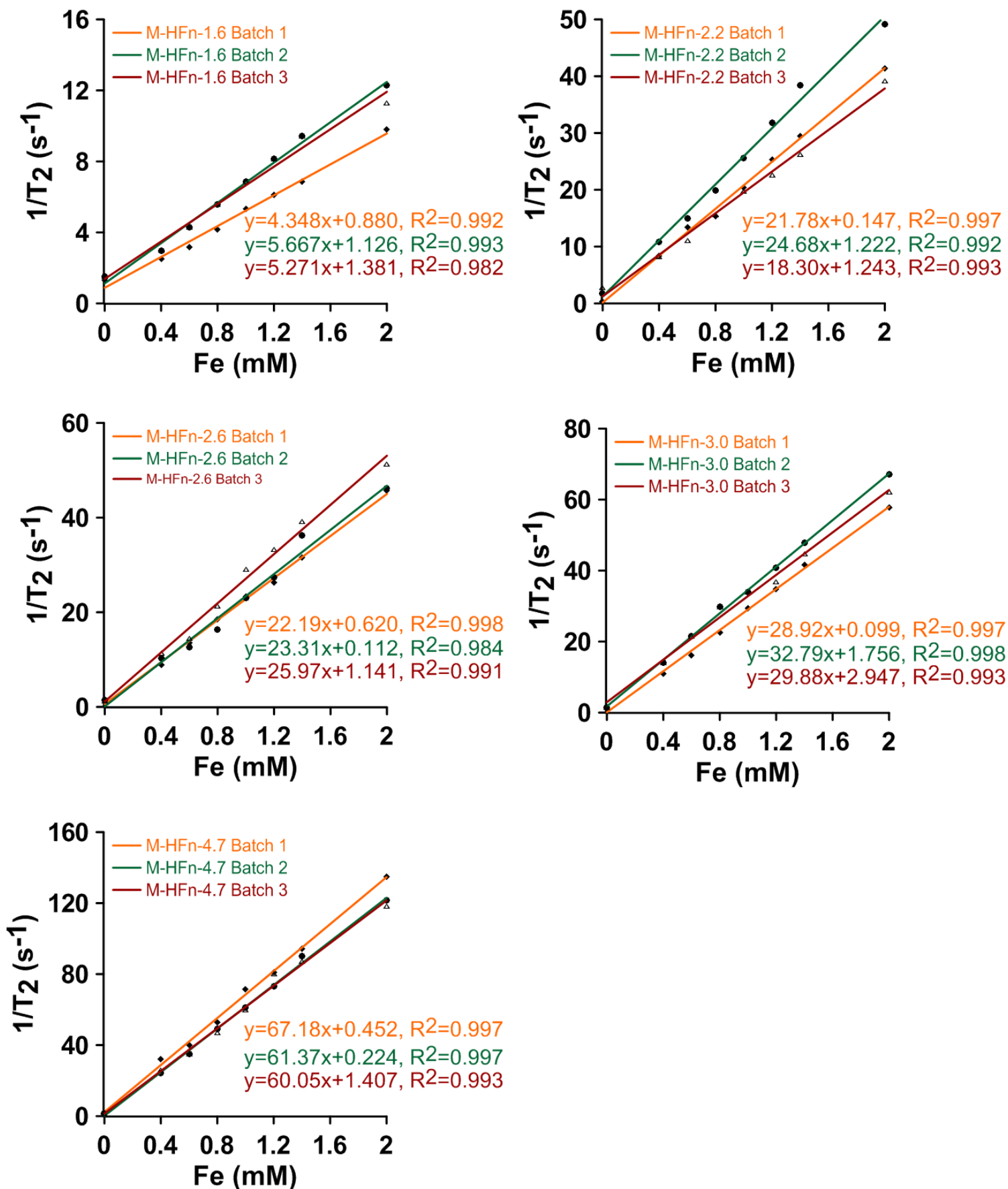


Fig. S8 Analysis of r_2 relaxivity of M-HFn nanoparticles by linear mapping iron concentration and relaxation rate.

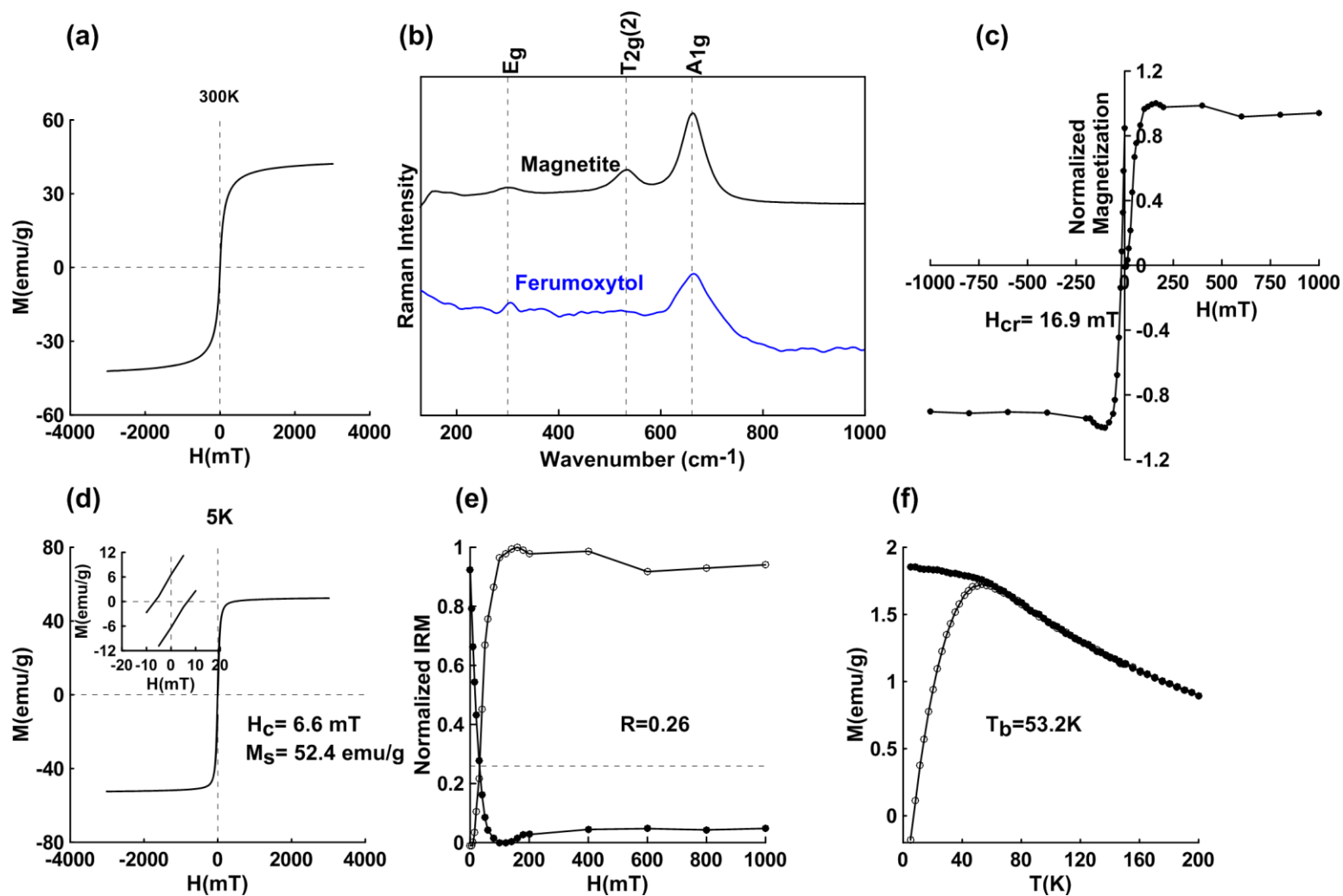


Fig. S9 Characterization of ferumoxytol. (a) Hysteresis loop measured at 300 K. (b) Raman spectrum analysis by comparing with a Raman spectrum of magnetite (reference R060191 in RRuFF database). (c) Normalized IRM acquisition curve and DC demagnetization curve. (d) 5 K Hysteresis loop, (e) the Wohlfarth-Cisowski test. (f) ZFC and FC curves, T_b of ferumoxytol here is 53.2 K.

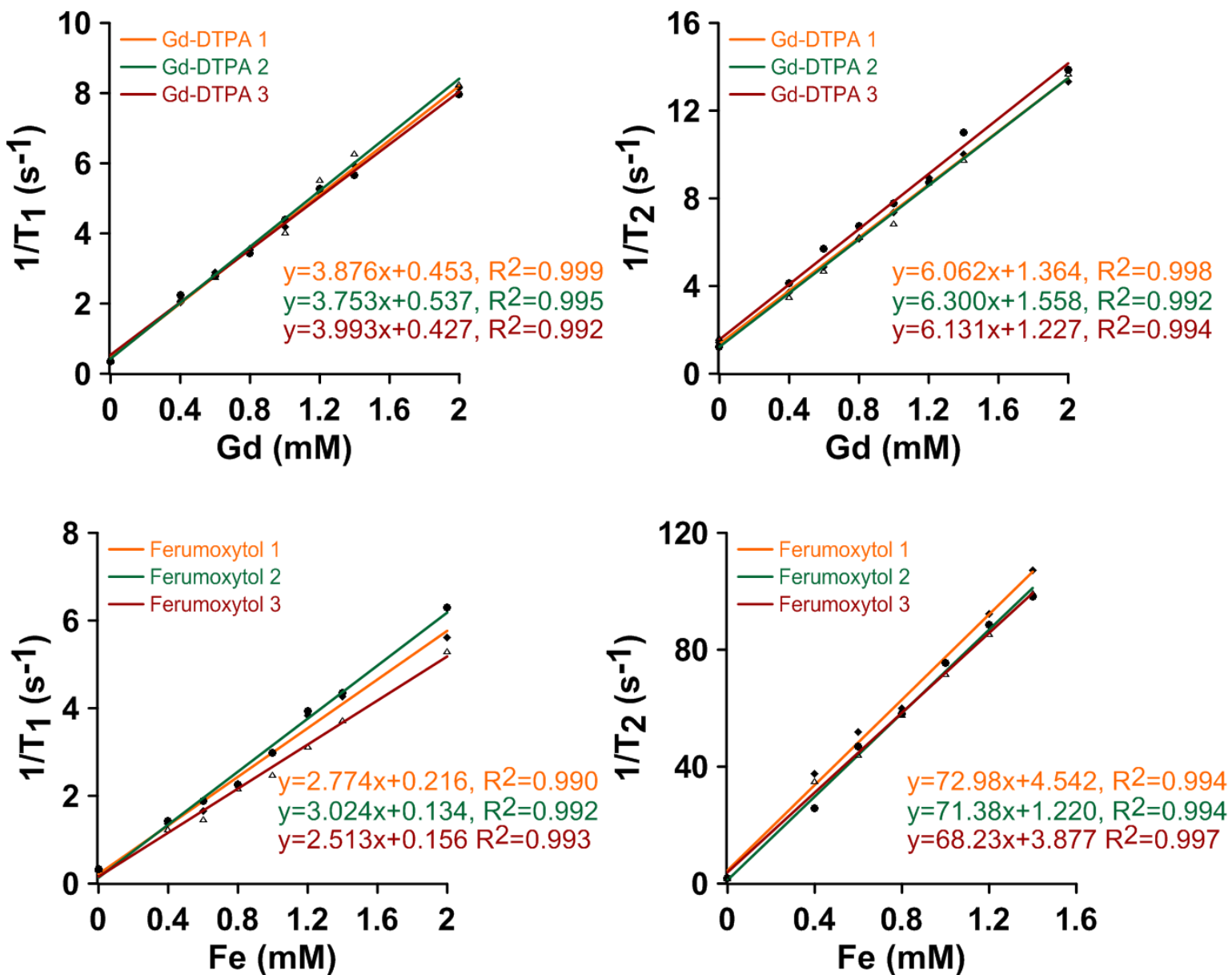


Fig. S10 Analysis of r_1 and r_2 relaxivity of Gd-DTPA and ferumoxytol at 7 T magnetic field.

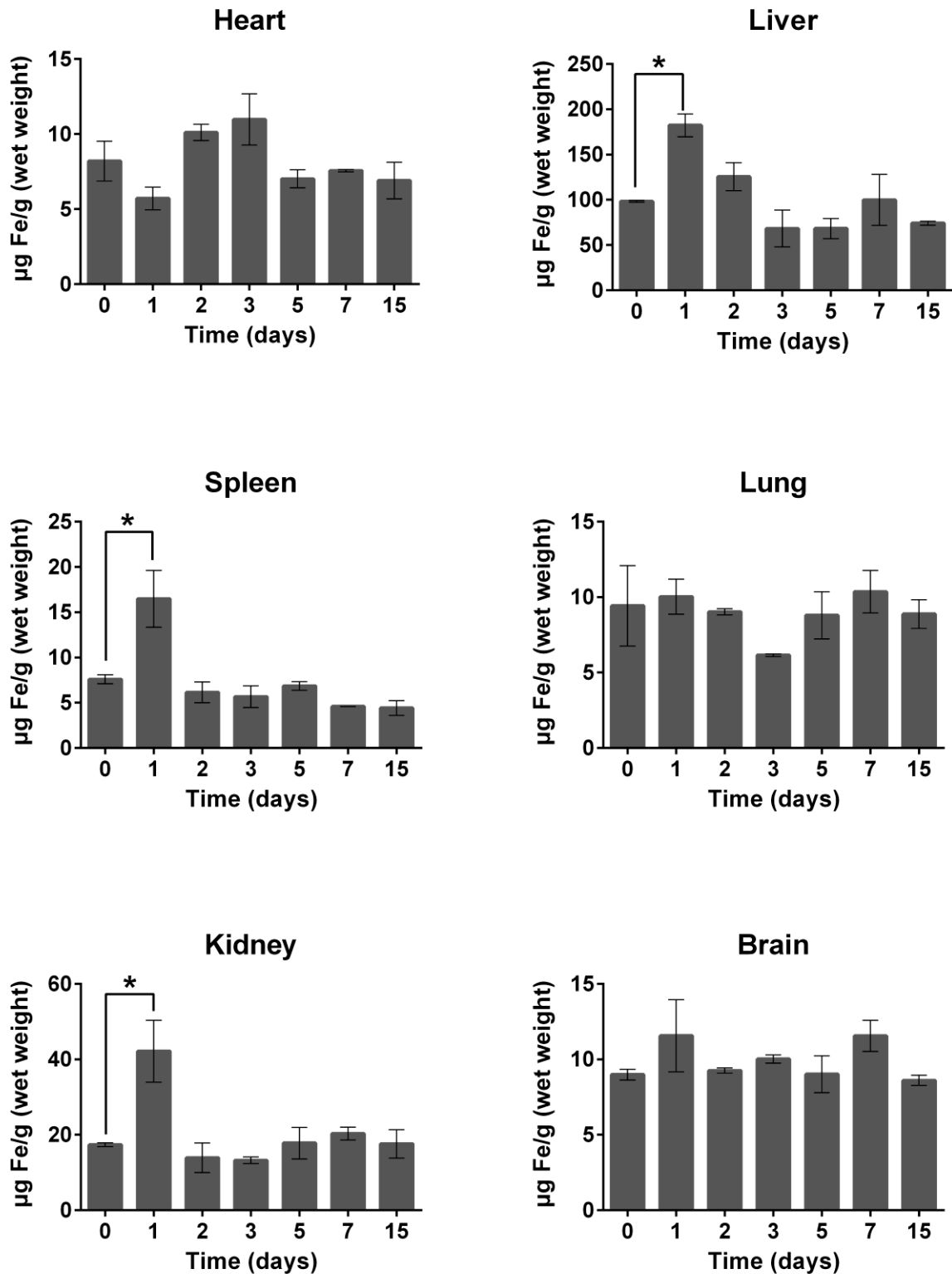


Fig. S11 Evaluation of iron accumulation in organs of mice post-injection with M-HFn-2.2. Heart, lung, brain do not show abnormal iron content from day 1 to day 15 after injection with M-HFn. While liver, spleen, kidney show a significant iron content increasing at 1 day post-injection but decrease to normal level from 2 days post-injection. (n = 3 mice in each time point, *P<0.05)